JOC The Journal of Organic Chemistry

Article

Diverse chemosensitizing 8,9-secolindenane-type sesquiterpenoid oligomers and monomers from Sarcandra glabra

Jun Chi, Shanshan Wei, Hongliang Gao, Dingqiao Xu, Lina Zhang, Lei Yang, Wenjun Xu, Jun Luo, and Ling-yi Kong

J. Org. Chem., **Just Accepted Manuscript** • DOI: 10.1021/acs.joc.9b00986 • Publication Date (Web): 13 Jun 2019

is published by the American Chemical Society. 1155 Sixteenth Street N.W., Washington, DC 20036

Diverse chemosensitizing 8,9-secolindenane-type sesquiterpenoid oligomers and monomers from *Sarcandra glabra*

Jun Chi, Shanshan Wei, Hongliang Gao, Dingqiao Xu, Lina Zhang, Lei Yang, Wenjun Xu, Jun Luo*, and Lingyi Kong*

Jiangsu Key Laboratory of Bioactive Natural Product Research and State Key Laboratory of Natural Medicines, School of Traditional Chinese Pharmacy, China Pharmaceutical University, Nanjing 210009, P. R. China

* Corresponding authors

E-mail: cpu_lykong@126.com

luojun@cpu.edu.cn

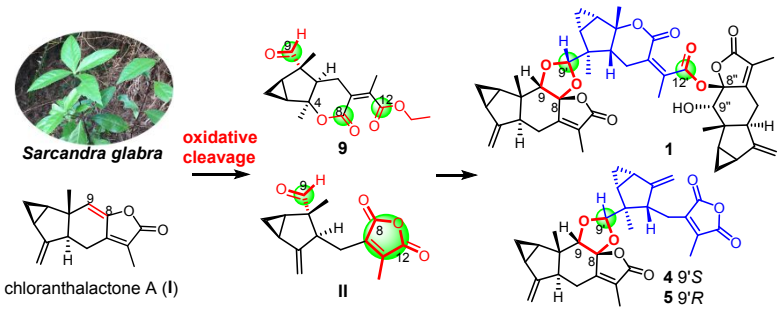

Abstract: The theoretical analysis and biomimetic conversion confirmed that the oxidative cleavage of the $\Delta^{8,9}$ double bond of chloranthalactone A (**I**), an abundant lindenane-type sesquiterpenoid in Chloranthaceae plants, generates 8,9-secolindenane (**II**) with active aldehyde and maleic anhydride fragments that can capture other fragments and produce oligomeric molecules. A careful phytochemical investigation of the leaves of *Sarcandra glabra* led to the discovery of eight novel 8,9-secolindenane-type sesquiterpenoid oligomers (sarglalactones A-H, compounds **1-8**), including three unprecedented trimers (**1-3**) and five unusual dimers (**4-8**), and five 8,9-secolindenane monomers (sarglalactones I-M, **9-13**). Their structures were determined by comprehensive HRMS, NMR, CD and X-ray diffraction analyses. Bioassay results showed that these oligomers significantly reversed the MDR of MCF-7/DOX cells and increased the sensitivity of U2 OS cells to doxorubicin by downregulating HMGB1 expression.

INTRODUCTION

Chloranthalactone A (**I**), also named shizukanolide B, was the first and most abundant lindenane-type sesquiterpenoid discovered in plants of the Chloranthaceae family.[1] Structurally, chloranthalactone A possesses a highly conjugated $\alpha,\beta,\gamma,\delta$-unsaturated lactone unit ($\Delta^{8,9}/\Delta^{7,11}$/CO-12) and a conjugation-preferred moiety ($\Delta^{4,15}$/C-5,6/$\Delta^{7,11}$/CO-12) that readily undergo oxidation, Diels-Alder, [2 + 2] cyclization and Michael addition reactions to construct complicated lindenane conjugates (Scheme S1).[2] Most of these molecules exhibit important bioactivities, including cytotoxic, anti-HIV, anti-inflammatory and antimalarial actions.[3] Their highly complex structures and potential bioactivities have attracted increasing interest from natural product and synthetic chemists, and the biomimetic synthesis of some structures has continuously been achieved in recent years.[4] In our previous study, a number of novel and anti-inflammatory lindenane monomers and oligomers based on monomer **I** were discovered from relevant Chloranthaceae plants.[5] By analyzing the changes in the C-C bonds of the reported structures, in addition to the [4 + 2] /[2 + 2] cycloaddition and Michael addition reactions, the oxidative cleavage of the $\Delta^{8,9}$ double bond in precursor **I** became our particular focus.[6] The oxidative reaction formed highly active 9-aldehyde and maleic anhydride moieties that function like the two arms of a person, which can catch other fragments to construct unprecedented molecules.

In this paper, the biomimetic oxidative cleavage of chloranthalactone A under O_2 and metal-free conditions generated 8,9-secolindenane (**II**), and a subsequent acetal reaction successfully produced the dimeric chlojapolactone A (**III**), the only 8,9-secolindenane-based oligomer reported from *Chloranthus japonicus* (Scheme 1).[7] The results of the biomimetic synthesis suggested that more rare and diverse oligomers based on 8,9-secolindenane (**II**) might be created in plants under physiological conditions. *Sarcandra glabra* (Thunb.) Nakai, which is widely distributed in southern Asia, is one of the renowned traditional Chinese medicines used for anti-inflammatory and adjuvant treatment for cancer.[8] According to our previous study, chloranthalactone A (**I**) and several of its derivatives exist in this plant,[1b,5b] and thus a detailed isolation of the leaves of *S. glabra* led to the discovery of eight 8,9-secolindenane-based oligomers (sarglalactones A-H, compounds **1**-**8**), including three unprecedented trimers and five unusual dimers, along with five 8,9-secolindenane monomers (sarglalactones I-M, **9**-**13**). Here, we report the characterization of these novel 8,9-secolindenane oligomers and their bioactivities by enhancing the sensitivity of MCF-7/DOX cells and U2 OS cells to doxorubicin (DOX).

RESULTS AND DISCUSSION

As mentioned above, the highly conjugated α, β, γ, δ-unsaturated lactone moiety enabled the $\Delta^{8,9}$ double bond of chloranthalactone A (**I**) to display a high reactivity,[9] and this compound was largely obtained from the seeds of *S. glabra* in our previous research.[5b] Thus, the biomimetic oxidation of precursor **I** was performed under atmosphere and visible light irradiation (Table S1-1 and Figure S1-2).[1b,10] As a result, the 8,9-epoxide chloranthalactone B (**IV**) was spontaneously formed with a yield of 80% over 30 days, and the trace C8-C9 cleavage product 8,9-secolindenane (**II**), which was previous semisynthesized from **I** through three step oxidations,[6a] was also measured using ^{1}H-NMR within 2 days (Figure S1-1). Furthermore, a variety of photocatalysts were employed to improve the yield of **II**.[11] Among these photocatalysts, 9-mesityl-10-methylacridinium perchlorate (Mes-Acr$^+$) showed the best transformation to product **II**, with a yield of 25%, and the reaction time was limited to 5 h.[12]

With 8,9-secolindenane (**II**) in hand, the biomimetic acetalization and alcoholysis reactions of its two active arms were designed and conducted (Scheme 1). Treatment of compound **II** with 10% *p*-TsOH and MeOH-H_2O (1:1, V:V) smoothly opened the maleic anhydride to yield chloranerectuslactone V (**IIa**), which was also reported in *Chloranthus erectus*.[6b] The epoxide **IV** was treated with 10% *p*-TsOH and DCM to produce a 91% yield of 8,9-diol chloranthalactone E (**IVa**),[13] which was unstable and existed as an epimeric mixture at C-8 due to the fast ketone-hemiacetal tautomerization.[14] After screening and optimization of the reaction conditions (Figure S1-3), chlojapolactone A (**III**) and 9′*R*-**III** were obtained as the acetalization dimers of 9-aldehyde **IIa** and 8,9-diol **IVa** at 30% and 4% yields following the application of 10% *p*-TsOH as an acid catalyst and molecular sieve in toluene to remove water at 100℃. Another trace product **IIIa**, was identified as an acetalized dimer of compounds **II** and **IVa** through an HPLC-HRMS analysis (Figures S1-4 and -5). Overall, the successful biomimetic syntheses of 8,9-secolindenanes and its oligomers confirmed our aforementioned hypothesis, and more diverse and unprecedented 8,9-secolindenane-based oligomers might be created by plants with abundant chloranthalactone A (**I**).

Scheme 1. Biomimetic conversion of chloranthalactone A (I).

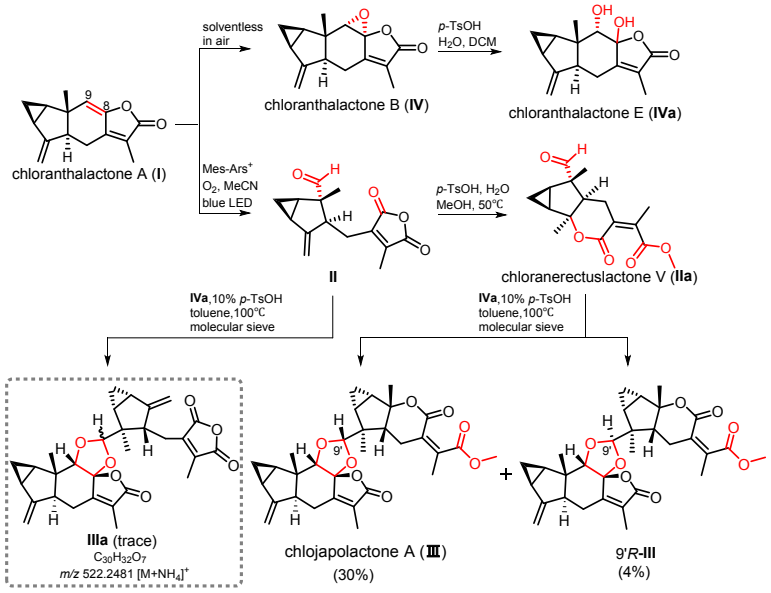

The air-dried and powdered leaves of *S. glabra* (4.6 kg) were exhaustively extracted with 95% EtOH under reflux. After removing the solvent, the residue (757.8 g) was successively extracted with petroleum ether and dichloromethane to obtain two extracts (150.1 g and 80.5 g, respectively). A detailed isolation of the petroleum ether fraction and small polar section of the dichloromethane fraction was conducted and led to the discovery of eight 8,9-secolindenane-type oligomers (sarglalactones A-H, **1-8**), including three unprecedented trimers and five unusual dimers, along with five 8,9-secolindenane monomers (sarglalactones I-M, **9-13**) (Figure 1).

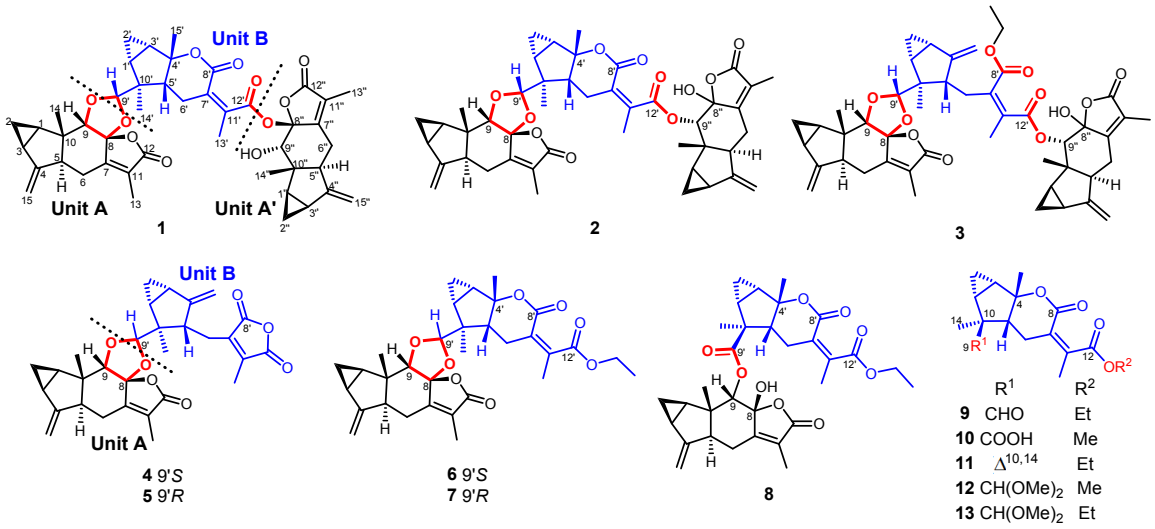

Figure 1. Structures of sarglalactones A-M (**1-13**).

Sarglalactone A (**1**), a white amorphous powder, was assigned the molecular formula of $C_{45}H_{50}O_{11}$ based on the HRMS data. Three pairs of characteristic upfield shifted methylene protons attributed to

the cyclopropane ring of lindenanes identified by evaluating ^{1}H NMR (Table 1) and 2D NMR (Figures 2 and 3) data indicated that compound **1** was an unprecedented lindenane trimer.[15] A careful analysis of its 1D and 2D NMR data indicated the presence of two 8,9-diol lindenanes [chloranthalactone E (**IVa**), units A and A′][13] and one 8,9-secolindenane [chloranerectuslactone V (**IIa**), unit B][6b]. The key HMBC correlations from the characteristic acetal methine H-9′ [δ_H 5.15 (s) and δ_C 109.7] to C-8 (δ_C 109.6) and H-9 at δ_H 4.31 (s) to C-9′ (δ_C 109.7) indicated that the aldehyde arm of unit B captured 8,9-diol unit A by acetalization.[7] The good agreement of chemical shifts of C-8″ at δ_C 105.6 and C-9″ at δ_H 4.18 (s) and δ_C 75.2 in unit A″ with those of C-8 in unit A and C-9 in diol **IVa**, as well as the "loose end" ester carbonyl of C-12′ (δ_C 166.8) of unit B, suggested that unit B caught unit A′ by esterification between OH-8″ and COOH-12′. The result was also supported by the lack of an HMBC correlation (Figure 2) of H-9″ /C-12′ and the tautomerism of 8,9-diol **IVa**. The key ROESY correlation (Figure 3) of H-9 /H-9′ of **1** revealed that these protons were located co-facially on the 1,3-dioxolane ring. The obvious differences in the chemical shifts of CH-5 [δ_H 3.42 (m) and δ_C 50.5] and CH_3-14 [δ_H 0.52 (s) and δ_C 17.3] in unit A and CH-5″ [δ_H 2.95 (dd, J = 13.3, 2.8 Hz) and δ_C 57.2] and CH_3-14″ [δ_H 0.78 (s) and δ_C 16.7] in unit A′ that were attributed to the anisotropy of the α, β-unsaturated lactone indicated that C-8-O-C-12 and H-14 were located co-facially and C-8″-O-C-12″ were located in the opposite direction to H-14″.[5d] The relative structure of **1** was further verified by the ROESY data (Figure 3). Therefore, the structure of **1** was determined as an unprecedented lindenane trimer arising from one 8,9-secolindenane core with two active arms to capture two 8,9-diol lindenanes by acetalization and esterification, respectively.

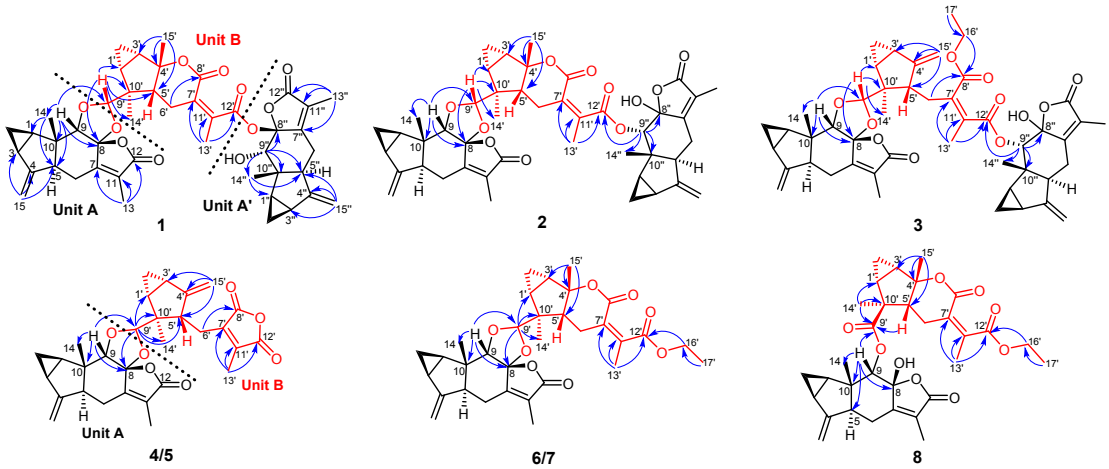

Figure 2. Key HMBC correlations of sarglalactones A-H (**1**-**8**).

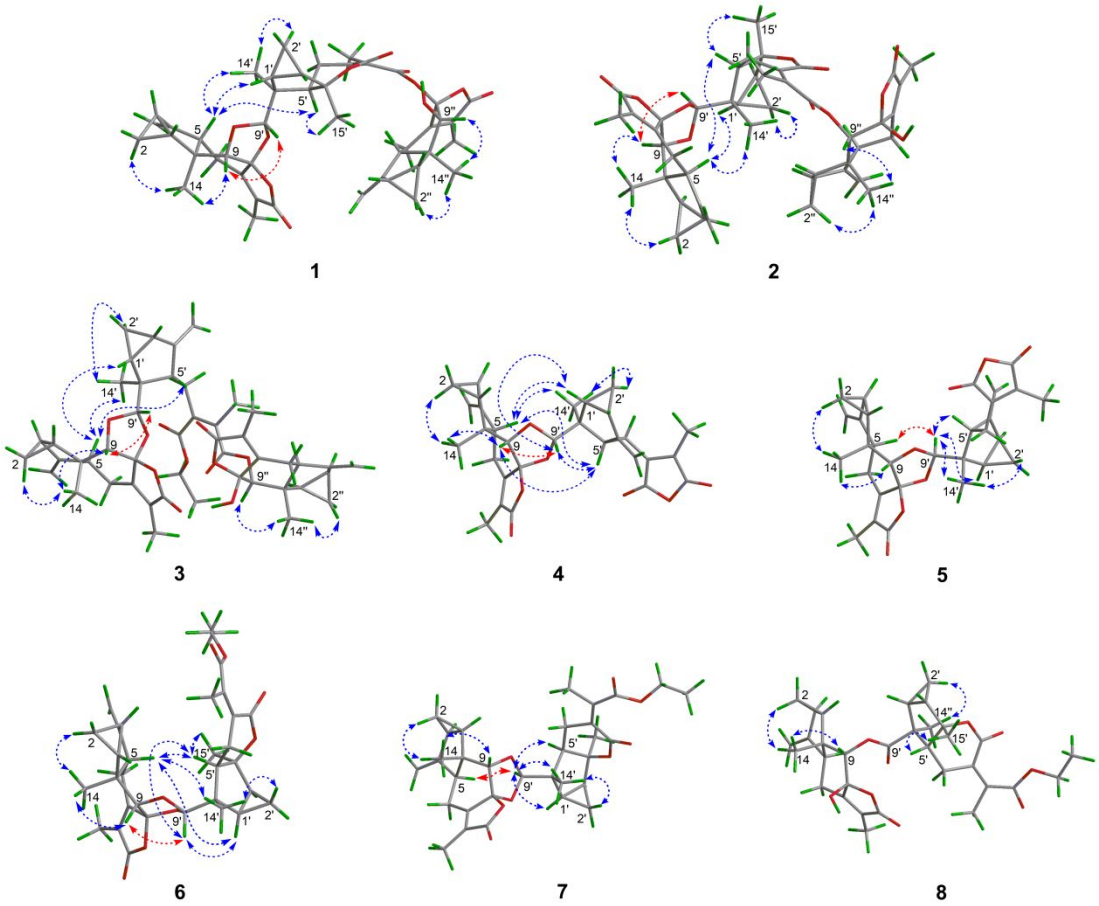

Figure 3. Key ROESY correlations of sarglalactones A-H (**1**-**8**).

The molecular formulas $C_{45}H_{50}O_{11}$ and $C_{47}H_{54}O_{11}$ of sarglalactones B (**2**) and C (**3**) obtained by HRMS spectra and the characteristic NMR data indicated that **2** and **3** were also two lindenane trimers. After a careful comparison, the NMR (Table S1-2) data of **2** was closely related to the data from **1**, reflecting the similarity of their structures. Two sets of NMR signals with a certain ratio were observed in Figures S2-31~35, and key HMBC correlations (Figure 2) from H-9″ [δ_H 5.18/5.56 (s)] of unit A′ to CO-12′ (δ_C 168.1/170.6) of unit B were present. These facts supported the connection of units B and A′ in **2** through esterification between COOH-12′ and OH-9″, as well as the existence of the tautomerization at C-8″ as monomer **IVa**. The NMR spectra of **3** was extremely similar to those of **2**, revealing that **3** was also a tautomeric 8,9-secolindenane trimer. One set of additional terminal double bond signals from C-15′ at δ_H 4.87/4.80 (s) and 4.63/4.54 (s) and δ_C 107.8 (Table S1-2), and HMBC correlations (Figure 2) from H_2-16′ [δ_H 4.20/4.10 (m)] to C-17′ (δ_C 13.8/13.9) and H_3-17′ [δ_H 1.20 (t, J = 7.1 Hz)] to C-16′ (δ_C 62.4/61.5) belonging to an ethoxy side chain, from H_2-16′ to CO-8′ (δ_C 168.2)

and from H-9″ [δ_H 5.16/5.50 (s)] to C-12′ (δ_C 168.7/168.8), indicated that the maleic anhydride arm of 8,9-secolindenane core (unit B) was esterified with ethanol and 8,9-diol lindenane moieties, respectively. The relative configurations of **2** and **3** were verified by the ROESY correlations and are shown in Figure 3.

Table 1. ^{1}H (600 MHz) and ^{13}C{^{1}H} (150 MHz) NMR data for 1 and 4 (δ in ppm, J in Hz, $CDCl_3$)

no.[a]	**1**						**4**			
	Unit A		Unit B		Unit A′		Unit A		Unit B	
	δ_H	δ_C	δ_H	δ_C	δ_H	δ_C	δ_H	δ_C	δ_H	δ_C
1	1.83 (m)	23.6	1.70 (m)	27.4	1.86 (m)	24.1	1.99 (m)	23.5	1.86 (m)	28.1
2	0.87 (m) 0.70 (m)	15.8	0.78 (m) 0.57 (q, 4.8)	8.0	0.90 (m) 0.78 (m)	15.8	0.83 (m) 0.67 (m)	15.7	0.82 (m) 0.71 (m)	11.2
3	1.97 (m)	23.7	1.63 (m)	29.5	1.86 (m)	23.0	1.84 (m)	23.7	1.90 (m)	25.0
4		151.3		93.2		150.4		151.8		153.5
5	3.42 (m)	50.5	2.31 (m)	47.1	2.95 (dd, 13.3, 2.8)	57.2	3.42 (m)	50.4	2.75 (dd, 12.4, 5.4)	44.4
6	2.51 (m) 2.27 (m)	22.3	2.42 (m) 2.07 (m)	26.3	2.62 (dd, 13.3, 2.8) 2.38 (m)	23.1	2.48 (dd, 17.8, 5.9) 2.23 (dd, 14.0,12.6)	22.3	2.54 (dd, 13.5, 5.6) 2.27 (dd, 13.5, 13.5)	28.2
7		154.2		125.1		155.8		154.6		143.5
8		109.6		166.3		105.6		109.7		165.8
9	4.31 (s)	85.4	5.15 (s)	109.7	4.18 (s)	75.2	4.26 (s)	85.3	5.08 (s)	109.4
10		42.8		49.0		42.2		42.8		48.1
11		128.0		139.5		126.6		125.8		142.0
12		171.2		166.8		171.7		171.4		166.2
13	1.87 (s)	8.9	1.95 (s)	17.0	1.91 (s)	8.9	1.84 (s)	8.8	2.01 (s)	10.3
14	0.52 (s)	17.3	1.12 (s)	16.1	0.78 (s)	16.7	0.48 (s)	17.3	1.26 (s)	15.5
15	5.00 (s) 4.74 (s)	106.8	1.58 (s)	36.1	5.00 (s) 4.76 (s)	106.7	5.04 (s) 4.71 (s)	106.5	4.90 (s) 4.33 (s)	107.7

[a] Numbers of carbon atoms in units A/B/A′ are represented as 1-15, 1′-15′, and 1″-15″, respectively.

The presence of 30-32 carbon atoms in the molecular formulas of sarglalactones D-H (**4**-**8**) by the HRMS spectra and the characteristic NMR data indicated that these compounds were lindenane dimers. A cyclic acetal linkage between units A and B in **4**-**7** was established by 9′-acetal methine at δ_H 5.08 (s) and δ_C 109.4 (Tables 1 and S1-3, only data for **4** are listed here) and the HMBC (Figure 2) correlations from H-9′ to C-8 (δ_C 109.7) and H-9 [δ_H 4.26 (s)] to C-9′. For compounds **4** and **5**, the presence of one set of maleic anhydride signals at δ_C 143.5/143.8 (C-7′), 165.8/165.9 (C-8′), 142.0/141.9 (C-11′), 166.2/166.3 (C-12′) and 10.3/10.2 (CH_3-13′) and terminal double bond signals of C-15′ at δ_H 4.90/4.92 (s) and 4.33/4.39 (s), and δ_C 107.7/107.3 in their 1D and 2D NMR spectra identified that **4**/**5** were the ones that conserved maleic anhydride units for 8,9-secolindenane core (unit B). Additionally, a comparative HPLC analyses of **IIIa** with the isolated compounds **4** and **5** (Figure S1-4) confirmed that the structure of trace product **IIIa** in biomimetic conversion section (Scheme 1) was sarglalactones D

(**4**). For compounds **6**/**7**, the observations of methyl signals from CH_3-15′ at δ_H 1.64/1.68 (s) and δ_C 31.3/30.8, an upfield shift of an oxyquaternary carbon of C-4′ at δ_C 92.6/93.1, and the key HMBC correlation from the ethoxy side chain H_2-16′ [δ_H 4.21/4.22 (m)] to the ester carbon C-12′ (δ_C 169.7/169.9) indicated that their 8,9-secolindenane cores existed as a lactone ring type that was similar to **1**/**2**. The identical HMBC correlations and obvious difference in the chemical shifts of C8/9/9′ suggested that **4**/**5** and **6**/**7** were two pair of epimers of an acetal carbon (C-9′), which was also confirmed by key ROESY correlations (Figure 3) of H-9/H-9′ in **4**/**6**, and H-5/H-9′ in **5**/**7**. For compound **8**, the absence of the characteristic acetal methine and obvious HMBC correlations between carbonyl carbon C-9′ (δ_C 176.0) and H-9 [δ_H 5.49 (s)] and H_3-14′ [δ_H 1.21 (s)] indicated that the common aldehyde arm was oxidized to a carboxyl group that captured one 8,9-diol-lindenane moiety (unit A) through esterification. The characteristic protons H-5 at δ_H 2.92 (m) and CH_3-14 at δ_H 1.07 (s) of **8** confirmed that the configuration of C-8 was consistent with the configuration of C-8″ in **1**. The relative structures of **4**-**8** were further verified by their ROESY data (Figure 3).

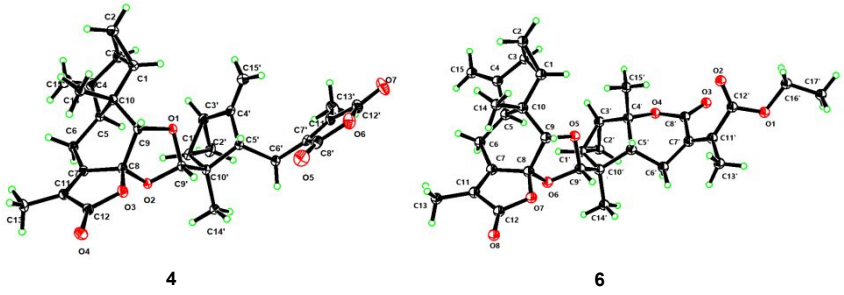

Figure 4. X-ray structures of sarglalactones D (**4**) and F (**6**).

The absolute configurations of compounds **1**-**7** were determined by combination of X-ray diffraction and circular dichroism analyses. Suitable crystals of **4** and **6** were finally obtained in methanol-water and acetone systems, respectively, and subjected to X-ray diffraction experiments. The Flack parameters of 0.00 (11) and 0.15 (11) for **4** and **6** (CCDC no 1893947 and 1893946) allowed the unambiguous assignments of their absolute configurations as 1*R*, 3*S*, 5*S*, 8*S*, 9*S*, 10*S*, 1′*R*, 3′*S*, 5′*S*, 9′*S*, 10′*S* and 1*R*, 3*S*, 5*S*, 8*S*, 9*S*, 10*S*, 1′*R*, 3′*S*, 4′*S*, 5′*R*, 9′*S*, 10′*S*, respectively (Figure 4). Furthermore, the CD spectra of **1**-**7** were detected in MeOH (Figure 5) and applied to resolve the stereochemistry of these oligomers. For epimers **6** and **7**, their curves displayed opposite exciton chirality in the 220-280 nm region dominated by the configurations of C-9′. An obvious negative Cotton effect at 253 nm ($\Delta\varepsilon$ -7.3) and a positive Cotton effect at 230 nm ($\Delta\varepsilon$ +6.4) were observed for **7**, indicating a anticlockwise

mode of two coupling *α,β*-unsaturated lactone chromophores and the 9′*R* configuration in **7** (Figure 1). The assignment of 9′*S*-configuration was also confirmed in **6** by its positive exciton chirality in the 220-280 nm region, as determined by X-ray diffraction. Accordingly, the absolute configurations of C-9′ in compounds **1-3** were determined to be *S* based on the similar Cotton effects in range of 220-280 nm as that in **6** (Figure 5). For compound **5**, its CD curve was in good agreement with that of **7** (Figure S1-8), although the absorption value at 231 nm of **5** (Δε -0.31) was not positive as that of **7** (Δε +6.4), which indicated the 9′*R* configuration in **5** as that in **7**. Thus, the absolute configurations of these oligomers were determined and shown in Figure 1.

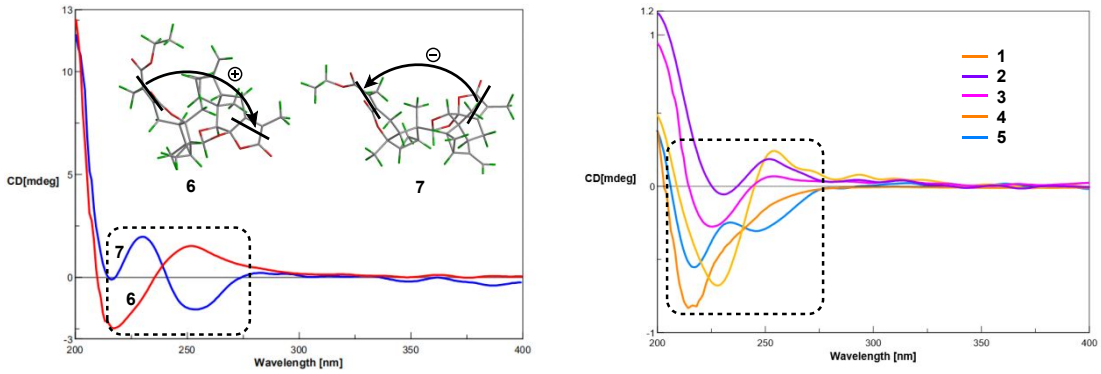

Figure 5. CD spectra of sarglalactones A-G (**1-7**) in MeOH.

According to the HRMS and $^{13}C\{^{1}H\}$-NMR data for sarglalactones I-M (**9-13**), these compounds contained 16-19 carbon atoms. Their 1D NMR (Table S1-4) data were similar to that of chloranerectuslactone V (**IIa**), indicating that they were also 8,9-secolindenanes. Structurally, compounds **10-13** were the oxidation, decarbonylation and acetalization derivatives of aldehyde **IIa** or **9**, as supported by the HMBC (Figure S1-9) correlations from H-1, H-5 and H-14 to the carboxyl group of C-9 (δ_C 181.4) of **10**, terminal double bond protons CH_2-14 at δ_H 5.08 (dd, J = 2.1 Hz) and 4.85 (s) to C-1, C-5 and C-10 (δ_C 153.2) of **11**, and two methoxy protons at δ_H 3.56 (s) to C-9 (δ_C 114.0) of **12** and **13**. In addition, a methoxy or ethoxyl group was attached to CO-12 of **9-13**, which was easily confirmed by the HMBC spectra. The relative structures of **9-13** were further verified by their ROESY data (Figure S1-9). Based on the CD spectra of **9** and **11** (Figure S1-10), the negative exciton chirality in 200-280 nm indicated a clockwise mode of two coupling chromophores and the absolute configurations of **9** and **11** were assigned as shown in Figure 1. In addition, monomer **9** with 9-aldehyde had a same 8,9-secolindenane unit of dimer **6** that have been identified by X-ray diffraction, and therefore the chemical conversion of **9** to **6** was performed using biomimetic acetalization

conditions described in Scheme 1. The HPLC and HPLC-HRMS analyses (Figures S1-11 and -12) indicated the formation of **6** from **9**, which confirmed the absolute configurations of **9** as 1′*R*, 3′*S*, 4′*S*, 5′*R,* 10′*S* (Figure 1). Limited by the amount of isolation, monomers **10** and **12-13** were confirmed to possess the identical absolute configurations as that of **9** with the biosynthesis consideration.

After isolation and identification, the bioactivities of these novel and diverse lindenane oligomers were screened. In an *in vitro* cytotoxicity assay*,* almost all the tested compounds were not cytotoxic toward MCF-7/DOX and U2OS cells (Table S1-5). However, compounds **1** and **4-8** potentially reversed the multidrug resistance of MCF-7/DOX cells, and the reversal fold values are shown in Table 2. Meanwhile, **1-8** showed significant synergistic cytotoxic effects in combination with DOX on U2 OS cells, and the combined indexes (CIs) were all less than 1 (Table 2). Based on the results, these oligomers increased the chemotherapeutic sensitivity of human tumor cells to doxorubicin. As reported, anticancer agents such as doxorubicin upregulate HMGB1 expression in U2 OS cells, and downregulation of HMGB1 expression restores the chemosensitivity of U2 OS cells.[16] Immunofluorescence staining revealed a reversal of HMGB1 expression in U2 OS cells following treatment with most of the compounds, as shown in Figure 6A. Western blots further revealed a concentration-dependent effect of **4** on decreasing HMGB1 levels in these cells to render them more sensitive to doxorubicin (Figure 6B).

Table 2. The *in vitro* MDR reversal activity and synergistic cytotoxicity of compounds 1-9.

Compounds	MDR reversal effects on MCF-7/DOX cells		Synergistic effects with doxorubicin on U2 OS cells (CI[c])
	IC_{50} (μM)[a]	RF value[b]	
Doxorubicin	156.0 ± 29.9		
1	2.7 ± 0.2	55.8	0.64 ± 0.08
2	-	-	0.92 ± 0.06
3	-	-	0.67 ± 0.07
4	6.9 ± 1.1	22.3	0.68 ± 0.06
5	13.2 ± 1.6	11.8	0.97 ± 0.06
6	3.4 ± 0.9	45.2	0.80 ± 0.06
7	1.2 ± 0.9	129.2	0.65 ± 0.08
8	8.1 ± 2.3	19.3	0.65 ± 0.05
9	> 50	-	1.24 ± 0.09
Verapamil[d]	13.7 ± 2.7	11.3	

[a] IC_{50}: 50% inhibitory concentration of DOX in the presence of **1** and **8** (10 μM), **4-7** (30 μM), and **9** (50 μM).
[b] The reversal fold (RF) value was calculated as follows: IC_{50} (DOX cells) /IC_{50} (DOX cells in the presence of isolates).
[c] The combined index (CI) value at 50% inhibition. According to the method described by Soriano et al.,[17] 1.1 ≤ CI ≤ 1.3 was considered as moderate antagonism, 0.9 ≤ CI < 1.1 as an additive effect, 0.8 ≤ CI < 0.9 as slight synergism, 0.6 ≤ CI < 0.8 as moderate synergism, 0.4 ≤ CI < 0.6 as synergism, and 0.2 ≤ CI <0.4 as strong synergism.
[d] Verapamil was used as a positive control (10 μM).

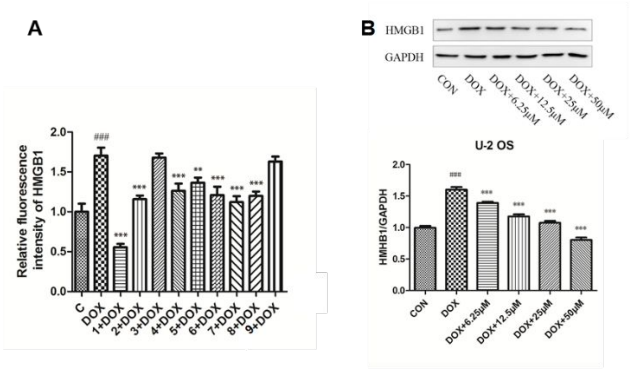

Figure 6. Inhibition of HMGB1 expression increased the sensitivity of U2 OS cells to doxorubicin *in vitro*. **A** Cells were treated with 50 μM isolates and 10 μM doxorubicin, and the expression levels of HMGB1 of compounds **1-9** were analyzed under high content microscope. **B** Cells were treated with different concentrations of **4** in combination with 10 μM doxorubicin, and HMGB1 expression was analyzed by Western blot assay.

CONCLUSIONS

In summary, a series of novel 8,9-secolindenanes and 8,9-secolindenane-based oligomers (compounds **1**-**13**) with effects on increasing chemosensitivity were successfully discovered in our current project guided by the strategy of theoretical prediction, biomimetic reaction verification, and detailed phytochemical investigations. These results also proved the effectiveness and practicality of this strategy for the discovery of valuable natural molecules from the plant kingdom. We believe that more interesting and valuable molecules are created by plants and are waiting to be discovered.

EXPERIMENTAL SECTION

General Experimental Details. Optical rotations were measured using a JASCO P-1020 polarimeter. The UV spectra were recorded using a UV-2450 UV/vis spectrophotometer. The CD spectra were recorded with a JASCO J-810 spectrometer. The IR measurements were performed using a Bruker Tensor 27 spectrometer. X-ray crystallographic data were collected with a Bruker Smart 1000

CCD diffractometer equipped with a graphite monochromator. The 1D and 2D NMR spectra were recorded using a Bruker Avance III NMR spectrometer with standard pulse sequences (^{1}H: 500 or 600 MHz, ^{13}C{^{1}H} NMR: 125 or 150 MHz) and TMS as an internal standard. High-resolution (HR)-ESI mass data were required with an Agilent 6520B UPLC-Q-TOF instrument. Column chromatography (CC) was performed with silica gel (Qingdao Haiyang Chemical Co., Ltd., Qingdao, China), MCI gel (Mitsubishi Chemical Industries Ltd., Japan), ODS (40-63 μm, Fuji, Japan), Sephadex LH-20 (Pharmacia, Sweden), and Toyoperal HW-40C (Tosoh Corporation, Japan). Preparative HPLC was performed using a Shimadzu LC-6AD series instrument with a Shim-park RP-C18 column (20 × 200 mm) and a Shimadzu SPD-20A detector.

Procedure for the Biomimetic Conversion of Chloranthalactone A (I).

*Chloranthalactone A (**I**).* Compound **I** (310.9 mg, 0.03 ‰) was provided as colorless oil from the fresh seeds of *S. glabra* (10 kg) in our previous study.[5b] ^{1}H NMR (600 MHz, $CDCl_3$) δ 1.66 (td, J = 7.6, 3.5 Hz, H-1), 0.92 (m H-2), 1.98 (m, H-3), 2.97 (dq, J = 13.3, 3.0 Hz, H-5), 2.70 (dd, J = 16.8, 3.0 Hz, H-6a), 2.27 (ddd, J = 16.8, 13.3, 2.5 Hz, H-6b), 6.25 (s, H-9), 1.90 (s, H-13), 0.79 (s, H-14), 5.06 (s, H-15a), 4.79 (s, H-15b); ^{13}C{^{1}H} NMR (150 MHz, $CDCl_3$) δ 26.6 (C-1), 17.1 (C-2), 22.6 (C-3), 150.2 (C-4), 62.2 (C-5), 21.5 (C-6), 148.2 (C-7), 149.7 (C-8), 120.0 (C-9), 40.2 (C-10), 122.6 (C-11), 171.3 (C-12), 8.8 (C-13), 22.3 (C-14), 106.7 (C-15). HRMS (ESI-TOF) m/z: $[M + H]^+$ Calcd for $C_{15}H_{17}O_2$ 229.1224; Found 229.1224.

*8,9-Seco-chloranthalactone A (**II**) and Chloranthalactone B (**IV**).* A solution of compound **I** (10.0 mg, 0.04 mmol) and Mes-Ars$^+$ (0.2 mg, 0.005 mmol) in dry ACN (2 ml) was irradiated with a 7 W blue LED under an oxygen atmosphere for 5 h. The resulting products were concentrated under reduced pressure. The residues were purified by using preparative TLC to afford **II** (2.3 mg, 23%) and **IV** (4.1 mg, 50%) as colorless oil. The details of the oxidation reaction of **I** to produce compounds **II** and **IV** under different conditions are shown in Table S1-1 and Figure S1-2.

Compound **II**: ^{1}H NMR (600 MHz, $CDCl_3$) δ 1.84 (ddd, J = 8.6, 5.5, 3.8 Hz, H-1), 0.97 (td, J = 8.6, 5.5 Hz, H-2a), 0.84 (dt, J = 5.5, 3.8 Hz, H-2b), 2.01 (ddd, J = 8.6, 5.5, 3.8 Hz, H-3), 2.94 (dd, J = 12.1, 5.3 Hz, H-5), 2.57 (dd, J = 13.3, 5.3 Hz, H-6a), 2.34 (dd, J = 13.3, 12.1 Hz, H-6b), 9.50 (s, H-9), 2.06 (s, H-13), 1.27 (s, H-14), 5.01 (s, H-15a), 4.46 (s, H-15b); ^{13}C{^{1}H} NMR (150 MHz, $CDCl_3$) δ 27.9 (C-1), 11.3 (C-2), 24.8 (C-3), 152.0 (C-4), 42.6 (C-5), 27.4 (C-6), 142.8 (C-7), 165.6 (C-8), 202.05 (C-9),

55.9 (C-10), 142.2 (C-11), 165.8 (C-12), 10.1 (C-13), 14.9 (C-14), 108.8 (C-15). HRMS (ESI-TOF) m/z: $[M + Na]^+$ Calcd for $C_{15}H_{16}O_4Na$ 283.0941; Found 283.0943.

Compound **IV**: ^1H NMR (500 MHz, $CDCl_3$) δ 1.71 (td, J = 8.0, 3.6 Hz, H-1), 0.97 (ddd, J = 9.1, 8.0, 5.5 Hz, H-2a), 0.84 (dt, J = 5.5, 3.6 Hz, H-2b), 1.99 (m, H-3), 3.38 (ddt, J = 13.0, 5.1, 2.0 Hz, H-5), 2.55 (ddq, J = 19.0, 5.1, 2.0 Hz, H-6a), 2.11 (ddq, J = 19.0, 13.0, 2.0 Hz, H-6b), 4.18 (s, H-9), 1.89 (s, H-13), 0.64 (s, H-14), 5.03 (s, H-15a), 4.70 (s, H-15b); $^{13}C\{^1H\}$ NMR (125 MHz, $CDCl_3$) δ 24.0 (C-1), 16.9 (C-2), 23.1 (C-3), 150.0 (C-4), 50.7 (C-5), 21.4 (C-6), 152.5 (C-7), 88.0 (C-8), 64.6 (C-9), 41.4 (C-10), 129.2 (C-11), 170.5 (C-12), 9.1 (C-13), 17.1 (C-14), 106.9 (C-15). HRMS (ESI-TOF) m/z: $[M + Na]^+$ Calcd for $C_{15}H_{16}O_3Na$ 267.0992; Found 267.0991.

*Chloranerectuslactone V (**IIa**)*. To a solution of **II** (50.2 mg, 0.19 mmol) in methanol (1 ml) was added dropwise an aqueous solution of *p*-TsOH (3.3 mg, 1 ml, 0.02 mmol). The solution was stirred in an oil bath at 50℃ using heating for 24 h. The resulting products were concentrated under reduced pressure. The residues were purified by using preparative TLC to afford **IIa** (45.9 mg, 83%) as a colorless oil. ^1H NMR (600 MHz, $CDCl_3$) δ 0.79 (m, H-2a), 0.73 (m, H-2b), 2.01 (ddd, J = 8.6, 5.5, 3.8 Hz, H-3), 2.65 (dd, J = 13.5, 6.4 Hz, H-5), 2.47 (dd, J = 13.5, 6.5 Hz, H-6a), 2.00 (m, H-6b), 9.60 (s, H-9), 1.99 (s, H-13), 1.21 (s, H-14), 1.54 (s, H-15), 3.78 (s, H-16). $^{13}C\{^1H\}$ NMR (150 MHz, $CDCl_3$) δ 27.4 (C-1), 7.5 (C-2), 29.1 (C-3), 91.8 (C-4), 44.1 (C-5), 25.6 (C-6), 127.2 (C-7), 166.5 (C-8), 202.2 (C-9), 56.9 (C-10), 139.2 (C-11), 170.4 (C-12), 15.8 (C-13), 16.5 (C-14), 31.8 (C-15), 52.9 (C-16). HRMS (ESI-TOF) m/z: $[M + Na]^+$ Calcd for $C_{16}H_{20}O_5Na$ 315.1203; Found 315.1204.

*Chloranthalactone E (**IVa**)*. Compound **IV** (11.0 mg, 0.04 mmol) was dissolved in 1 ml of acetonitrile/water (5:1). The solution was stirred at room temperature for 48 h. The resulting product was concentrated under reduced pressure. The residue was purified by using preparative TLC to afford **IVa** (2.1 mg, 20%) as crystalline solid. To **IV** (10.5 mg, 0.04 mmol) in 1 ml of DCM was added aqueous solution of *p*-TsOH (8.7 mg, 0.2 ml, 0.05 mmol) dropwise manner. The solution was stirred at room temperature for 2 h. The resulting product was concentrated under reduced pressure. The residue was purified using preparative TLC to afford **IVa** (9.6 mg, 91%) as crystalline solid. 8α-OH /8β-OH-**IVa**: ^1H NMR (500 MHz, $CDCl_3$) δ 1.99/1.90 (m, H-1), 0.81 (td, J = 8.6, 5.1 Hz, H-2a)/0.92 (q, J = 4.2 Hz, H-2a), 0.84 (q, J = 5.1 Hz, H-2b)/0.79 (m, H-2b), 1.99 /1.90 (m, H-3), 3.38 (ddt, J = 12.2, 6.1, 2.8 Hz, H-5) /2.96 (dq, J = 13.2, 2.8 Hz, H-5), 2.51 (m H-6a), 2.22 (dd, J = 17.8, 12.2 Hz, H-6b)/2.12 (t, J

= 13.2 Hz, H-6b), 3.94 (s, H-9)/4.12 (s, H-9), 1.80/1.81 (s, H-13), 0.53/0.95 (s, H-14), 4.99 (s, H-15a), 4.70/4.72 (s, H-15b); $^{13}C\{^{1}H\}$ NMR (125 MHz, $CDCl_3$) δ 23.1/24.3 (C-1), 15.8/16.1 (C-2), 23.9/23.0 (C-3), 152.1/150.9 (C-4), 51.6/57.1 (C-5), 22.4 (C-6), 159.7/159.3 (C-7), 104.8/105.9 (C-8), 76.3 (C-9), 43.5/42.2 (C-10), 124.9/124.3 (C-11), 173.9/173.6 (C-12), 8.4/8.5 (C-13), 20.1/16.5 (C-14), 106.4/106.1 (C-15). HRMS (ESI-TOF) m/z: $[M + Na]^+$ Calcd for $C_{15}H_{18}O_4Na$ 285.1097; Found 285.1099.

*Chlojapolactone A (**III**) and 9′R-**III***. To a solution of **IIa** (27.80 mg, 0.095 mmol) and **IVa** (50.12 mg, 0.191 mmol) in 2 ml toluene were added with 10% *p*-TsOH solution (8.22 mg, 0.03 mmol) and molecular sieve. The solutions were stirred in an oil bath at 100℃ or room temperature. The resulting products were reverse extracted with H_2O, and mother liquors were retained and concentrated under reduced pressure. The residue was purified by using preparative TLC to afford **III** (15.33 mg, 30%) and 9′*R*-**III** (1.82 mg, 4%) as amorphous solids. The details for the acetal reaction of compounds **II** and **IV** under different conditions are shown in Figure S1-4.

Compound **III**: ^{1}H NMR (500 MHz, $CDCl_3$) δ 1.81 (m, H-1), 0.84 (m, H-2a), 0.68 (m, H-2b), 1.81 (m, H-3), 3.41 (m, H-5), 2.50 (dd, *J* = 18.2, 6.9 Hz, H-6a), 2.26 (dd, *J* = 18.2, 12.6 Hz, H-6b), 4.29 (s, H-9), 1.84 (s, H-13), 0.49 (s, H-14), 5.01 (s, H-15a), 4.71 (s, H-15b), 1.69 (m, H-1′), 0.70 (m, H-2′a), 0.56 (m, H-2′b), 1.99 (m, H-3′), 2.31 (dd, *J* = 12.5, 6.8 Hz, H-5′), 2.44 (dd, *J* = 13.3, 6.8 Hz, H-6′a), 1.99 (t, *J* = 13.2 Hz, H-6′b), 5.14 (s, H-9′), 1.95 (s, H-13′), 1.13 (s, H-14′), 1.61 (s, H-15′). $^{13}C\{^{1}H\}$ NMR (125 MHz, $CDCl_3$) δ 23.7 (C-1), 15.7 (C-2), 23.6 (C-3), 151.2 (C-4), 50.4 (C-5), 22.2 (C-6), 154.3 (C-7), 109.8 (C-8), 85.3 (C-9), 42.8 (C-10), 127.9 (C-11), 171.1 (C-12), 8.8 (C-13), 17.2 (C-14), 106.8 (C-15), 27.6 (C-1′), 7.8 (C-2′), 29.4 (C-3′), 92.7 (C-4′), 48.3 (C-5′), 27.3 (C-6′), 128.4 (C-7′), 167.3 (C-8′), 109.8 (C-9′), 49.0 (C-10′), 138.0 (C-11′), 170.2 (C-12′), 16.3 (C-13′), 16.5 (C-14′), 31.2 (C-15′) , 52.7 (C-16′). HRMS (ESI-TOF) m/z: $[M + Na]^+$ Calcd for $C_{31}H_{36}O_8Na$ 559.2302; Found 559.2301.

9′*R*-**III**: ^{1}H NMR (600 MHz, $CDCl_3$) δ 1.97 (m, H-1), 0.89 (m, H-2a), 0.76 (q, *J* = 4.0 Hz, H-2b), 2.02 (m, H-3), 3.15 (m, H-5), 2.61 (ddd, *J* = 18.3, 6.5, 2.4 Hz, H-6a), 2.27 (dd, *J* = 18.2, 12.4 Hz, H-6b), 4.37 (s, H-9), 1.84 (s, H-13), 0.50 (s, H-14), 5.07 (s, H-15a), 4.77 (s, H-15b), 1.58 (m, H-1′), 0.71 (td, *J* = 8.5, 6.0 Hz, H-2′a), 0.57 (td, *J* = 6.0, 4.2 Hz, H-2′b), 1.99 (m, H-3′), 2.44 (dd, *J* = 12.5, 6.9 Hz, H-5′), 2.49 (dd, *J* = 12.5, 6.9 Hz, H-6′a), 1.95 (m, H-6′b), 5.55 (s, H-9′), 2.05 (s, H-13′), 1.08 (s, H-14′), 1.68

(s, H-15′); $^{13}C\{^{1}H\}$ NMR (150 MHz, $CDCl_3$) δ 22.8 (C-1), 16.2 (C-2), 23.9 (C-3), 150.8 (C-4), 53.4 (C-5), 22.2 (C-6), 154.6 (C-7), 110.3 (C-8), 88.0 (C-9), 51.6 (C-10), 126.7 (C-11), 171.0 (C-12), 8.8 (C-13), 18.4 (C-14), 107.1 (C-15), 28.4 (C-1′), 7.8 (C-2′), 29.6 (C-3′), 93.2 (C-4′), 46.8 (C-5′), 27.8 (C-6′), 129.2 (C-7′), 168.1 (C-8′), 115.4 (C-9′), 43.6 (C-10′), 137.7 (C-11′), 170.1 (C-12′), 16.2 (C-13′), 17.6 (C-14′), 30.8 (C-15′), 52.7 (C-16′). HRMS (ESI-TOF) m/z: $[M + Na]^+$ Calcd for $C_{31}H_{36}O_8Na$ 559.2301; Found 559.2301.

*Acetalization of Compounds **II** and **IVa***. Following the above procedure, the reactants were **II** (2.50 mg, 0.010 mmol), **IVa** (5.00 mg, 0.019 mmol), and 0.001 mmol *p*-TsOH, HCOOH, or HAc in 2 ml of toluene. The mixtures were dissolved in MeOH and detected by using HPLC (Figure S1-5). The product from the reaction with 10 mol% *p*-TsOH was detected by using LC/MS (Figure S1-6), and the molecular formula of compound **IIIa** was assigned as $C_{30}H_{32}O_7$ based on the pseudomolecular ion at *m/z* 522.2481 $[M+NH_4]^+$ (calcd for $C_{30}H_{33}NO_7$, 522.2486).

Plant Material. The leaves of *Sarcandra glabra* (Thunb.) Nakai were collected from Guangxi Province in China in September 2016 and were identified by Professor Mian Zhang of China Pharmaceutical University. A voucher specimen (No. SG201609) was deposited in the Department of Natural Medicinal Chemistry, China Pharmaceutical University.

Extraction and Isolation. The petroleum ether (150.1 g) fraction was separated using silica gel CC and eluted with a gradient of DCM-MeOH (1:0, 100:1, 50:1 and 25:1, v/v) to afford seven fractions (Fr. A~G) based on a TLC analysis. Fr. D (35.1 g) and Fr. E (50.4 g) were successively subjected to separation with an HW-40C gel eluted with DCM-MeOH (1:1) to afford Fr. D-1-~7 and Fr. E-1~2. Fr. D-6 (2.8 g) was applied to a LH-20 gel (DCM-MeOH, 1:1) and further purified using preparative HPLC with 85% MeOH-H_2O to obtain **4** (128.2 mg) and **5** (6.5 mg). Fr. E-2 was subjected to MCI gel, eluted with MeOH-H_2O (30%, 50%, 70%, and 90%) to afford nine subfractions: Fr. E-2-1~9. Then, Fr. E-2-7 (3.5 g) and Fr. E-2-8 (5.6 g) were separately submitted to separation on an LH-20 gel with MeOH and then purified by using preparative HPLC to yield **1** (7.2 mg), **2** (21.2 mg), **3** (13.5 mg), **6** (105.3 mg), **7** (5.1 mg), **8** (4.0 mg) and **10** (2.0 mg). The dichloromethane (80.5 g) fraction was separated on silica gel CC and eluted with a gradient of DCM-MeOH (1:0, 50:1, 25:1 and 0:1 v/v) to afford five fractions (Fr. a~e) based on a TLC analysis. Fr. b (5.0 g) was subjected to separation on an

HW-40C gel, LH-20 gel and preparative HPLC to yield **9** (33.2 mg), **11** (8.2 mg), **12** (1.9 mg) and **13** (2.6 mg).

Spectroscopic Data of Isolated Compounds.

*Sarglalactone A (**1**):* white amorphous powder; $[\alpha]_D^{26}$ -35.6 (*c* 0.12, MeOH); IR (KBr) ν_{max} 3435, 2924, 1776, 1602, 1094, 975 cm^{-1}; UV (MeOH) log (ε) λ_{max} 200 (4.54) nm; CD (MeOH) λ ($\Delta\varepsilon$) 228 (-0.71), 253 (+0.44); for ^1H (600 MHz) and $^{13}C\{^1H\}$ (150 MHz) NMR data, see Table 1; HRMS (ESI-TOF) m/z: $[M + Na]^+$ Calcd for $C_{45}H_{50}O_{11}Na$ 789.3245; Found 789.3240.

*Sarglalactone B (**2**):* white amorphous powder; $[\alpha]_D^{26}$ -13.2 (*c* 0.49, MeOH); IR (KBr) ν_{max} 3432, 2925, 1770, 1096, 975 cm^{-1}; UV (MeOH) (log ε) λ_{max} 209 (4.34) nm; CD (MeOH) λ ($\Delta\varepsilon$) 230 (-0.20), 251 (+0.42); for ^1H (600 MHz) and $^{13}C\{^1H\}$ (150 MHz) NMR data, see Table S1-2; HRMS (ESI-TOF) m/z: $[M + Na]^+$ Calcd for $C_{45}H_{50}O_{11}Na$ 789.3245; Found 789.3242.

*Sarglalactone C (**3**):* white amorphous powder; $[\alpha]_D^{26}$ 17.6 (*c* 0.20, MeOH); IR (KBr) ν_{max} 3368, 2925, 1773, 1662, 1254, 1176, 1100, 973 cm^{-1}; UV (MeOH) log (ε) λ_{max} 210 (4.48) nm; CD (MeOH) λ ($\Delta\varepsilon$) 221 (-0.94), 253 (+0.47); for ^1H (600 MHz) and $^{13}C\{^1H\}$ (150 MHz) NMR data, see Table S1-2; HRMS (ESI-TOF) m/z: $[M + Na]^+$ Calcd for $C_{47}H_{54}O_{11}Na$, 817.3558; Found 817.3558.

*Sarglalactone D (**4**):* colorless needle crystals; mp 204-207 ºC; $[\alpha]_D^{26}$ -56.8 (*c* 0.27, $CHCl_3$); IR (KBr) ν_{max} 2968, 1765, 1277, 1103, 968, 926, 867 cm^{-1}; UV ($CHCl_3$) (log ε) λ_{max} 203 (4.29) nm; CD (MeOH) λ ($\Delta\varepsilon$) 213 (-5.59); for ^1H (600 MHz) and $^{13}C\{^1H\}$ (150 MHz) NMR data, see Table 1; HRMS (ESI-TOF) m/z: $[M + Na]^+$ Calcd for $C_{30}H_{32}O_7Na$ 527. 2040; Found 527.2041.

*Sarglalactone E (**5**):* white amorphous powder; $[\alpha]_D^{26}$ -20.8 (*c* 0.05, MeOH); IR (KBr) ν_{max} 3393, 2922, 1770, 1384, 1279, 1102, 978 cm^{-1}; UV (MeOH) log (ε) λ_{max} 203 (4.27) nm; CD (MeOH) λ ($\Delta\varepsilon$) 216 (-0.84), 231 (-0.31), 246 (-0.44); for ^1H (500 MHz) and $^{13}C\{^1H\}$ (125 MHz) NMR data, see Table S1-3; HRMS (ESI-TOF) m/z: $[M + Na]^+$ Calcd for $C_{30}H_{32}O_7Na$ 527.2040; Found 527.2043.

*Sarglalactone F (**6**):* colorless needle crystals; mp 112-115 ºC; $[\alpha]_D^{26}$ -66.8 (*c* 0.20, MeOH); IR (KBr) ν_{max} 2981, 1778, 1730, 1307, 1269, 1183, 1091, 976 cm^{-1}; UV (MeOH) (log ε) λ_{max} 210 (4.31) nm; CD (MeOH) λ ($\Delta\varepsilon$) 218 (-1.03), 252 (+0.62); for ^1H (500 MHz) and $^{13}C\{^1H\}$ (125 MHz) NMR data, see Table S1-3; HRMS (ESI-TOF) m/z: $[M + Na]^+$ Calcd for $C_{32}H_{38}O_8Na$ 573.2459; Found 573.2462.

*Sarglalactone G (**7**):* white amorphous powder; $[\alpha]_D^{26}$ -88.6 (*c* 0.25, MeOH); IR (KBr) ν_{max} 2971, 2929, 1774, 1728, 1306, 1264, 1178, 1143, 1101, 1084, 976 cm^{-1}; UV (MeOH) log (ε) λ_{max} 210 (4.28)

nm; CD (MeOH) $\lambda(\Delta\varepsilon)$ 230 (+6.4), 253 (-7.3); for ^{1}H (500 MHz) and ^{13}C{^{1}H} (125 MHz) NMR data, see Table S1-3; HRMS (ESI-TOF) m/z: $[M + Na]^+$ Calcd for $C_{32}H_{38}O_8Na$ 573.2459; Found 577.2461.

*Sarglalactone H (**8**):* white amorphous powder; $[\alpha]_D^{26}$ 22.1 (*c* 0.16, MeOH); IR (KBr) ν_{max} 2925, 2853, 1733, 1593, 1461, 1384, 1310, 1172, 1103 cm^{-1}; UV (MeOH) (log ε) λ_{max} 207 (4.20) nm; CD (MeOH) λ ($\Delta\varepsilon$) 242 (+5.26); for ^{1}H (500 MHz) and ^{13}C{^{1}H} (125 MHz) NMR data, see Table S1-3; HRMS (ESI-TOF) m/z: $[M + Na]^+$ Calcd for $C_{32}H_{38}O_9Na$ 589.2408; Found 589. 2407.

*Sarglalactone I (**9**):* colorless oil; $[\alpha]_D^{27}$ -19.1 (*c* 0.1, MeOH); IR (KBr) ν_{max} 3449, 2977, 1729, 1640, 1386, 1273,1085 cm^{-1}; UV (MeOH) log (ε) λ_{max} 208 (3.86) nm; CD (MeOH) λ ($\Delta\varepsilon$) 211 (-5.57), 236 (+15.8); for ^{1}H (600 MHz) and ^{13}C{^{1}H} (150 MHz) NMR data, see Table S1-4; HRMS (ESI-TOF) m/z: $[M + Na]^+$ Calcd for $C_{17}H_{22}O_5Na$ 329.1359; Found 329.1361.

*Sarglalactone J (**10**):* colorless oil; $[\alpha]_D^{27}$ 22.6 (*c* 0.20, MeOH); IR (KBr) ν_{max} 3451, 1722, 1650, 1384, 1314, 1087, 1038 cm^{-1}; UV (MeOH) (log ε) λ_{max} 203 (3.88) nm; for ^{1}H (600 MHz) and ^{13}C{^{1}H} (150 MHz) NMR data, see Table S1-4; HRMS (ESI-TOF) m/z: $[M + Na]^+$ Calcd for $C_{16}H_{20}O_6Na$ 331.1152; Found 311.1150.

*Sarglalactone K (**11**):* colorless oil; $[\alpha]_D^{27}$ 8.4 (*c* 0.11, MeOH); IR (KBr) ν_{max} 3446, 2924, 1733, 1637, 1384, 1266, 1100 cm^{-1}; UV (MeOH) log (ε) λ_{max} 208 (3.86) nm; CD (MeOH) λ ($\Delta\varepsilon$) 211 (-8.47), 252 (+2.8); for ^{1}H (500 MHz) and ^{13}C{^{1}H} (125 MHz) NMR data, see Table S1-4; HRMS (ESI-TOF) m/z: $[M + H]^+$ Calcd for $C_{16}H_{21}O_4$ 277.1434; Found 277.1432.

*Sarglalactone L (**12**):* colorless oil; $[\alpha]_D^{27}$ -16.6 (*c* 0.01, MeOH); IR (KBr) ν_{max} 3449, 2923, 1637, 1384, 1080 cm^{-1}; UV (MeOH) (log ε) λ_{max} 203 (3.88) nm; for ^{1}H (500 MHz) and ^{13}C{^{1}H} (125 MHz) NMR data, see Table S1-4; HRMS (ESI-TOF) m/z: $[M + Na]^+$ Calcd for $C_{18}H_{26}O_6Na$ 361.1622; Found 361.1622.

*Sarglalactone M (**13**):* colorless oil; $[\alpha]_D^{27}$ -16.7 (*c* 0.16, MeOH); IR (KBr) ν_{max} 3454, 1725, 1639, 1384, 1307, 1271, 1181,1082 cm^{-1}; UV (MeOH) log (ε) λ_{max}: 208 (3.86) nm; for ^{1}H (600 MHz) and ^{13}C{^{1}H} (150 MHz) NMR data, see Table S1-4; HRMS (ESI-TOF) m/z: $[M + Na]^+$ Calcd for $C_{19}H_{28}O_6Na$ 375.1778; Found 375.1778.

X-ray Crystallographic Analysis.

The signal crystals of **4** ($C_{30}H_{32}O_7$) and **6** ($C_{32}H_{38}O_8$) were obtained from MeOH/H_2O (10:1) and acetone solutions, respectively. Suitable crystals were selected and then measured using a Bruker

APEX-II CCD diffractometer with Cu Kα radiation. Crystal data for compound **4** (M = 504.56 g/mol): orthorhombic, space group $P2_12_12_1$ (no. 19), a = 7.5297(6) Å, b = 18.5627(15) Å, c = 18.7260(15) Å, V = 2617.4(4) Å^3, Z = 4, T = 150 K, μ(CuKα) = 0.741 mm^{-1}, *Dcalc* = 1.280 g/cm^3, 42067 reflections measured ($6.7^\circ \leq 2\Theta \leq 131.98^\circ$), 4499 unique ($R_{int}$ = 0.0431, R_{sigma} = 0.0169) which were used in all calculations. The final R_1 was 0.0278 (>2 sigma (I)) and wR_2 was 0.0711 (all data). Crystal data for compound **6** (M = 550.62 g/mol): monoclinic, space group $P2_1$ (no. 4), a = 7.510(5) Å, b = 35.163(11) Å, c = 10.914(3) Å, β = 91.743(14)°, V = 2881(2) Å^3, Z = 4, T = 220.0 K, μ(CuKα) = 0.741 mm^{-1}, *Dcalc* = 1.270 g/cm^3, 37278 reflections measured ($5.026^\circ \leq 2\Theta \leq 142.172^\circ$), 9954 unique ($R_{int}$ = 0.0685, R_{sigma} = 0.0636) which were used in all calculations. The final R_1 was 0.0473 ($I > 2\sigma(I)$) and wR_2 was 0.1154 (all data). The crystallographic data for compounds **4** and **6** have been deposited in the Cambridge Crystallographic Data Centre (Nos. 1893947 and 1893946, respectively) and are included in the Supporting Information.

Cytotoxicity Assays. MCF-7/DOX and U2OS cells were cultured in RPMI-1640 medium supplemented with 10% fetal bovine serum, harvested with trypsin, and resuspended at a final density of 4.5 × 104 cells/ml. Aliquots (0.1 ml) of cell suspensions were seeded evenly into 96-well culture plates and incubated in a 37 °C incubator with a 5% CO_2 atmosphere for 24 h. A series of concentrations of the compounds in DMSO were added to designated wells. After 48 h, an MTT assay was performed as described previously.[18]

MDR Reversal Assays. MCF-7/DOX cells were distributed into 96-well culture plates at a density of 4.5 × 103 cells per well. A full range of concentrations of doxorubicin with or without 30 or 10 μM compounds or 10 μM verapamil (positive control) were added to the cells. After 48 h, the MTT assay was performed as described above. IC_{50} values for doxorubicin were calculated from plotted results by setting untreated cells to 100%. The reversal fold, in terms of potency of reversal, was calculated using the following formula: reversal fold (RF) = IC_{50} (MCF-7/DOX cells)/IC_{50} (MCF-7/DOX cells in combination with compounds). All assays were performed in triplicate. [18]

Synergistic Cytotoxicity Assays.

MTT Growth Assay to Evaluate the Synergistic Effect. U2 OS cells were cultured in RPMI-1640 medium supplemented with 10% fetal bovine serum, harvested with trypsin, and resuspended at a final density of 4.5 × 104 cells/ml. A full range of concentrations of doxorubicin with or without 50 μM

compounds were added to the cells. After 48 h, the MTT assay was performed as described above. Synergistic effects of the compounds and doxorubicin were quantified by calculating the combined index (CI) using the following equation: $CI = D_A/IC_{50,\ A} + D_B/IC_{50,\ DOX}$. $IC_{50,\ A}$ and $IC_{50,\ DOX}$ were the doses of the test compound and doxorubicin that produced 50% inhibition alone, respectively; D_A and D_{DOX} were the doses of the test compound and doxorubicin that produced 50% inhibition in the combination system, respectively.[19]

High Content Imaging to Detect the Levels of HMGB1. Immunofluorescence staining was performed using a previously described method.[20] U2 OS cells were cultured on a 96-well glass-bottom culture plate. Then, 10 μM doxorubicin with or without 50 μM compounds were added to the cells and incubated for 48 h. Cells were fixed with warm 4% paraformaldehyde for 15 min at room temperature. Next, the fixative was removed, and cells were washed with PBS 3 times for 5 min each. Cells were permeabilized with 0.5% Triton X-100 for 10 min and blocked with 5% BSA for 60 min. Cells were incubated with primary antibodies against HMGB1 (diluted with 5% BSA at 1:400) overnight at 4 °C. After the incubation, cells washed with PBS 3 times for 5 min each. Cells were then incubated with an Alexa Fluor-conjugated secondary antibody for 1.5 h at room temperature in the dark. Afterwards, cells were washed with PBS 3 times for 5 min each. The nuclei were stained with DAPI (Beyotime, Haimen, China) for 10 min before imaging. Images were captured using an ImageXpressei Micro High Content (Molecular Devices, USA).

Western blot analysis. Western blot analyses were performed as previously described.[22] U2 OS cells and their corresponding parental cells were incubated with various concentrations of compound **3** and 10 μM DOX, or 0.1% DMSO for 48 h. Cells were harvested by trypsinization and treated with 1× RIPA lysis buffer (50 mM Tris-HCl, pH 7.4, 150 mM NaCl, 0.25% deoxycholic acid, 1% NP-40, 1 mM EDTA and protease inhibitors) (Amresco, Solon, USA) to extract the total proteins. An aliquot of proteins from the total cell lysates (30 to 40 μg/lane) was separated by using sodium dodecyl sulfate (8%, 12% or 15%) polyacrylamide gel electrophoresis (SDS–PAGE, Bio-Rad Laboratories, Hercules, CA), wet-transferred to NC membranes (Bio-Rad Laboratories, Hercules, CA), blotted with primary antibodies against cleaved HMGB1, and probed with secondary isotype-specific antibodies conjugated to horseradish peroxidase (Cell Signaling Technology). Bound immuno-complexes were detected using a ChemiDOC™ XRS+system (Bio-Rad Laboratories, Hercules, CA).

ASSOCIATED CONTENT

Supporting Information

The Supporting Information is available free of charge on the ACS Publications website.

Spectroscopic data including 1D and 2D NMR and HRMS spectra of synthetic and isolated compounds; NMR, HPLC and LC-MS analyses of biomimetic conversion; Cytotoxicity of isolated compounds (PDF)

Crystallographic data of compounds **4** and **6** (CIF)

AUTHOR INFORMATION

Corresponding Author

* E-mail: cpu_lykong@126.com

* E-mail: luojun@cpu.edu.cn

ORCID

Lingyi Kong: 0000-0001-9712-2618

Jun Luo: 0000-0002-7892-011X

Notes

The authors declare no competing financial interest.

ACKNOWLEDGEMENTS

This study was supported in part by grants from the National Natural Science Foundation of China (81430092 and 81673554), the Outstanding Youth Fund of the Basic Research Program of Jiangsu Province (BK20160077), the "Double First-Class" University Project (CPU2018GY08), the 111 Project from Ministry of Education of China and the State Administration of Foreign Export Affairs of China (B18056), and the Drug Innovation Major Project (2018ZX09711-001-007).

REFERENCES

(1) (a) Nozoe, S.; Uchida, M.; Kusano, G.; Kondo, Y.; Takemoto, T. Two New Sesquiterpenoids from *Chloranthus glaber* Makino. *Heterocycles* **1978**, *9*, 139-144. (b) Tsui, W. Y.; Brown, G. D. Cycloeudesmanolides from *Sarcandra glabra*. *Phytochemistry* **1996**, *43*, 819-821.

(2) (a) Takeda, Y.; Yamashita, H.; Matsumoto, T.; Terao. H. Chloranthalactone F, a Sesquiterpenoid from the Leaves of *Chloranthus glaber*. *Phytochemistry* **1993**, *33*, 713-715. (b) Kawabata, J.; Fukushi,

Y.; Tahara, S.; Mizutani, J. Shizukaol A, a Sesquiterpene Dimer from *Chloranthus japonicus*. *Phytochemistry* **1990**, *29*, 2332-2334. (c) Kawabata, J.; Fukushi, E.; Mizutani, J. Symmetric Sesquiterpene Dimer from *Chloranthus serratus*. *Phytochemistry* **1993**, *32*, 1347-1349. (d) Lucia, A.; Sauvain, M.; Beck, S.; Moulis, C.; Gimenez A.; Jullian, V. Bolivianine, a New Sesquiterpene with an Unusual Skeleton from *Hedyosmum angustifolium*, and Its Isomer, Isobolivianine. *Org. Lett.* **2007**, *9*, 4693-4696.

(3) (a) Ni, G.; Zhang, H.; Liu, H. C.; Yang, S. P.; Geng, M. Y.; Yue, J. M. Cytotoxic Sesquiterpenoids from *Sarcandra glabra*. *Tetrahedron* **2013**, *69*, 564-569. (b) Fang, P. L.; Cao, Y. L.; Yan, H.; Pan, L. L.; Liu, S. C.; Gong, N. B.; Lü, Y.; Chen, C. X.; Zhong, H. M.; Guo, Y. Lindenane Disesquiterpenoids with Anti-HIV-1 Activity from *Chloranthus japonicus*. *J. Nat. Prod*. **2011**, *74*, 1408-1413. (c) Wang, P.; Luo, J.; Zhang, Y. M.; Kong, L. Y. Sesquiterpene Dimers Esterified with Diverse Small Organic Acids from the Seeds of *Sarcandra glabra. Tetrahedron* **2015**, *46*, 5362-5370. (d) Zhou, B.; Yan, W.; Dalal, S.; Merino, E. F.; Liu, Q. F.; Xu, C. H.; Tao, Y.; Jian, D.; Kingston, D. G. I.; Cassera, M. B.; Yue, J. M. Nanomolar Antimalarial Agents against Chloroquine-Resistant *Plasmodium falciparum* from Medicinal Plants and Their Structure–Activity Relationships. *J. Nat. Prod.* **2017**, *80*, 96-107.

(4) (a) Yuan, C.; Du, B.; Deng, H.; Yi, M.; Liu, B. Total Syntheses of Sarcandrolide J and Shizukaol D: Lindenane Sesquiterpenoid [4+2] Dimers. *Angew. Chem. Int. Ed.* **2017**, *56*, 637-640. (b) Wu, J. L.; Lu, Y. S.; Tang, B.; Peng, X. S. Total Syntheses of Shizukaols A and E. **2018**, *9*, 4040-4046. (c). Yang G. X., Ma G. L., Li H., Huang T., Xiong J., Hu J. F. Advanced Natural Products Chemistry Research in China between 2015 and 2017. *Chin J. Nat. Med.* **2018**, *16*, 0881-0906.

(5) (a) Chi, J.; Xu, W. J.; Wei, S. S.; Wang, X. B.; Li, J. X.; Gao, H. L.; Kong, L. Y.; Luo, J. Chlotrichenes A and B, Two Lindenane Sesquiterpene Dimers with Highly Fused Carbon Skeletons from *Chloranthus holostegius*. *Org. Lett.* **2019**, *21*, 789-792. (b) Wang, P.; Li, R. J.; Liu, R. H.; Jian, K. L.; Yang, M. H.; Yang, L.; Kong, L. Y.; Luo, J. Sarglaperoxides A and B, Sesquiterpene-Normonoterpene Conjugates with a Peroxide Bridge from the Seeds of *Sarcandra glabra*. *Org. Lett.* **2016**, *18*, 832-835.

(6) (a) Sumioka, H.; Harinantenaina, L.; Matsunami, K.; Otsuka, H.; Kawahata, M.; Yamaguchi, K. Linderolides A–F, Eudesmane-type Sesquiterpene Lactones and Linderoline, a Germacrane-type

Sesquiterpene from the Roots of *Lindera strychnifolia* and Their Inhibitory Activity on NO Production in RAW 264.7 Cells *in Vitro*. *Phytochemistry* **2011**, *72*, 2165-2171. (b) Huong, T. T.; Thong, N. V.; Minh, T. T.; Tram, L. H.; Anh, N. T.; Cuong, H. D.; Cuong, P. V.; Ca, D. V. Chloranerectuslactone V (I), a New Sesquiterpene from *Chloranthus erectus* Verdc. *Lett. Org. Chem.* **2014**, *11*, 639-642.

(7) Guo, Y. Q.; Tang, G. H.; Li, Z. Z.; Lin, S. L.; Yin, S. Chlojapolactone A, an Unprecedented 1,3-Dioxolane Linked-lindenane Sesquiterpenoid Dimer from *Chloranthus japonicus*. *RSC Adv.* **2015**, *5*, 103047-103051.

(8) (a) Xia, N. H.; Joël, J. *Flora of China*; Science Press: Beijing, **1999**, *4*, 132. (b) Chinese Pharmacopoeia Committee. *Pharmacopoeia of People's Republic of China, Part 1*. The Medicine Science and Technology Press of China, **2015**, 223-224. (c) Tsai, Y. C.; Chen, S. H.; Lin, L. C.; Fu, S. L. Anti-inflammatory Principles from *Sarcandra glabra*. *J Agric Food Chem.* **2017**, *65*, 6497-6505.

(9) Monnier, J. R.; Peters, K. T.; Hartley, G. W. The selective epoxidation of conjugated olefins containing allylic substituents and epoxidation of propylene in the presence of butadiene. *J. Catal*. **2004**, *225*, 374-380.

(10) Bryliakov, K. P. Catalytic Asymmetric Oxygenations with the Environmentally Benign Oxidants H_2O_2 and O_2. *Chem. Rev.* **2017**, *117*, 11406 −11459.

(11) (a) Margaros, I.; Montagnon, T.; Tofi, M.; Pavlakos, E.; Vassilikogiannakis, G. The power of singlet oxygen chemistry in biomimetic syntheses. *Tetrahedron* **2006**, *62*, 5308-5317. (b) Vassilikoginanakis, G.; Stratakis, M. Biomimetic Total Synthesis of Litseaverticillols A, C, D, F, and G: Singlet-Oxygen-Initiated Cascades & dagger. *Angew. Chem.* **2003**, *115*, 5623-5626.

(12) Wang, K.; Meng, L. G.; Zhang, Q.; Wang, L. Direct Construction of 4-aryl Tetralones via Visible-light-induced Cyclization of Styrenes with Molecular Oxygen. *Green Chem.* **2016**, *18*, 2864–2870.

(13) Masaaki, U.; Yutaka, K.; Genjiro, K.; Yoshikazu, K.; Shigeo, N.; Chizuko, K.; Tsunematsu, T. Studies on the Constituents of *Chloranthus* spp.Ⅲ. Six Sesquiterpenes from *Chloranthus japonicus*. *Chem. Pharm. Bull.* **1980**, *28,* 92-102.

(14) (a) Zhang, C. X.; Wang, C. C.; Wang, Z. H.; Tanabe, G.; Muraoka, O.; Lin, A. J.; Xu, J. Y.; Wu X. M.; Wu, L.; Xie, W. J. Total Synthesis, Structural Elucidation and Anti-inflammatory Activity Evaluation of 2-deoxy-3,6-anhydro Hexofuranoside Derivatives Isolated from *Sauropus rostratus. Org.*

Biomol. Chem. **2016***, 14*, 10906-10913. (b) Camougis, G.; Takman, B. H.; Rene, J.; Tasse, P. Potency difference between the zwitterion form and the cation forms of tetrodotoxin. *Science* **1967**, *156*, 1625-1627.

(15) Zhou, B.; Liu, Q. F.; Dalal, S.; Cassera, M. B.; Yue, J. M. Fortunoids A-C, Three Sesquiterpenoid Dimers with Different Carbon Skeletons from *Chloranthus fortuna*. *Org. Lett.* **2017**, *19*, 734-737.

(16) Huang, J.; Ni, J.; Liu, K.; Yu, Y.; Xie, M.; Kang, R.; Vernon, P.; Cao, L.; Tang, D. HMGB1 Promotes Drug Resistance in Osteosarcoma. *Cancer Res.* **2012**, *72*, 230-238.

(17) Soriano, A. F.; Helfrich, B.; Chan, D. C.; Heasley, L. E.; Jr, B. P.; Chou, T. C. Synergistic Effects of New Chemopreventive Agents and Conventional Cytotoxic Agents against Human Lung Cancer Cell Lines. *Cancer Res.* **1999**, *59*, 6178-6184.

(18) Yang, L.; Wei, D. D.; Chen, Z.; Wang, J. S.; Kong, L. Y. Reversal of Multidrug Resistance in Human Breast Cancer Cells by *Curcuma wenyujin* and *Chrysanthemum indicum*. *Phytomedicine*. **2011**, *18*, 710-718.

(19) Yang, J.; Liu, R. H. Synergistic Effect of Apple Extracts and Quercetin 3-*β*-D-glucoside Combination on Antiproliferative Activity in MCF-7 Human Breast Cancer Cells *in vitro*. *J. Agric. Food Chem.* **2009**, *57*, 8581 -8586.

(20) Fujimoto, D.; Ueda, Y.; Hirono, Y.; Goi, T.; Yamaguchi, A. PAR1 Participates in the Ability of Multidrug Resistance and Tumorigenesis by Controlling Hippo-YAP Pathway. *Oncotarget*. **2015**, *6*, 34788-34799.

(21) Xia, Y. Z.; Yang, L.; Wang, Z. D.; Guo, C.; Zhang, C.; Geng, Y. D.; Kong, L. Y. Schisandrin A Enhances the Cytotoxicity of Doxorubicin by the Inhibition of Nuclear Factor-kappa B Signaling in a Doxorubicin-resistant Human Osteosarcoma Cell Line. *Rsc Adv.* **2015**, *5*, 13.